Journal of Magnetic Resonance **149,** 126–130 (2001)
doi:10.1006/jmre.2001.2288, available online at http://www.idealibrary.com on IDEAL®

# *In Vivo* $^{31}$P Echo-Planar Spectroscopic Imaging of Human Calf Muscle

Thomas Wilhelm and Peter Bachert[1]

*Abteilung Biophysik und Medizinische Strahlenphysik, Deutsches Krebsforschungszentrum (dkfz), D-69120 Heidelberg, Germany*

Received August 21, 2000; revised December 29, 2000

**Localized phosphorus-31 NMR spectra of human calf muscle** *in vivo* **were obtained by means of echo-planar spectroscopic imaging (EPSI) with a 1.5-T whole-body scanner. The technique permits the measurement of two-dimensional $^{31}$P SI data at a minimum acquisition time of 2.4 s (8 × 8 voxels, TR = 300 ms). With 9.4 min measurement time (TR = 1100 ms, 64 averages) and 25 × 25 × 40 mm spatial resolution** *in vivo* **the $^{31}$P NMR signal-to-noise ratio ($S/N$) of the phosphocreatine (PCr) resonance was about 45; the multiplets of nucleoside 5′-triphosphates were resolved. Spectral quality permits quantitative assessment of the PCr signal in a measurement time that is shorter by a factor of 2 or more than the minimum measurement time feasible with chemical-shift imaging. In a functional EPSI study with a time resolution of 20.5 s on the calf muscle of volunteers, spectra showed a 40% decrease of the PCr signal intensity (at rest: $S/N \cong 12$) upon exertion of the muscle.** © 2001 Academic Press

*Key Words*: **phosphorus NMR; echo-planar spectroscopic imaging; human calf muscle.**

## INTRODUCTION

Echo-planar imaging (EPI), proposed in mid-1970s (*1*), is the fastest clinically used MR imaging method. EPI is now widely applied to functional MRI studies in whole-body scanners (*2, 3*). Echo-planar-based techniques permit fast spectroscopic imaging (*4, 5*) and were implemented for volume-selected water-suppressed proton NMR spectroscopy of the human brain *in vivo* (*6*). This approach is called EPSI (echo-planar spectroscopic imaging) and samples gradient echoes in contrast to TSI (turbo spectroscopic imaging) techniques which acquire multiple spin echoes (*7*). A theoretical evaluation and comparison of fast SI techniques was given recently by Pohmann *et al.* (*8*).

Chemical-shift imaging (CSI, *9*) has become a standard technique of localized *in vivo* $^{31}$P NMR spectroscopy of human brain, liver, and skeletal muscle. $^{31}$P CSI can detect compounds with short spin–spin relaxation times, in particular nucleoside 5′-triphosphates (NTP) with $T_2$ in the range of 74–93 ms ($\alpha$-, $\gamma$-NTP) in human calf muscle *in vivo* at 1.5 T (*10*). Since the $T_2$ of phosphocreatine (PCr) is quite long ($T_2 \cong 425$ ms (*10*)), fast spectroscopic imaging of this compound could be feasible. EPSI of phosphorus-containing metabolites has, to our knowledge, not been considered so far. Therefore, the purpose of this study was to explore an EPSI approach for *in vivo* $^{31}$P NMR with a 1.5-T whole-body tomograph.

## RESULTS

The pulse sequence applied in two-dimensional (2D) $^{31}$P EPSI experiments is displayed in Fig. 1. Figure 2a shows the $^{31}$P signal-to-noise ratio ($S/N$) as a function of dwell time (DW) in EPSI experiments with an aqueous solution of phosphocreatine (50 mM). Owing to the reconstruction routine employed $DW = 4\times$ gradient rise time ($T_{\text{ramp}}$). $S/N$ was in the range of 12–20 for a measurement time of 5.9 min, and declined with increasing DW. With fast gradient switching (DW < 1 ms) data were unstable, indicating technical limitations. For $T_{\text{ramp}} < 150$ $\mu$s the supervision software of the scanner detected the limit of possible physiological stimulation and stopped the measurement.

Results of EPSI experiments with multiple interleaves are displayed in Fig. 2b together with EPSI and CSI data obtained with the same experimental setup. The interleaved acquisition technique increased the spectral bandwidth, but did not improve $S/N$.

Figures 3a and 3b show $^{31}$P NMR spectra from EPSI and CSI studies, respectively, with the 50 mM PCr model solution. In both experiments 64 spectra were obtained with field of view FOV = $(300\text{ mm})^2$ in a measurement time of 5.9 min. The sensitivity of the PCr resonance of the EPSI spectrum is $(S/N)_{\text{E}} \cong 35$ (Fig. 3a; repetition time TR = 1100 ms, $N = 8$ phase-encoding steps, number of averages NA = 40), while in the CSI spectrum $(S/N)_{\text{C}} \cong 50$ (Fig. 3b; TR = 1100 ms, $N \times N = 8 \times 8$, NA = 5). Spectral widths were 1 kHz ($T_{\text{ramp}} = 250$ $\mu$s) in the EPSI experiment (Fig. 3a) and 4 kHz (DW = 250 $\mu$s) in the CSI experiment (Fig. 3b; a 1-kHz section of the spectrum is displayed).

Figure 3c shows a transversal $^{31}$P echo-planar spectroscopic image (grid resolution: 25 mm) of the phantom with overlay of the contour obtained by $^{1}$H MRI to demonstrate the extent of voxel bleeding. Comparison of EPSI and corresponding CSI map (not shown) indicated the same spatial resolution and signal contamination.

[1] To whom correspondence should be addressed at Abteilung Biophysik und Medizinische Strahlenphysik (E0200), Deutsches Krebsforschungszentrum (dkfz), Im Neuenheimer Feld 280, D-69120 Heidelberg, Germany. Fax: ++49-6221-422531. E-mail: p.bachert@dkfz-heidelberg.de.



1090-7807/01 $35.00

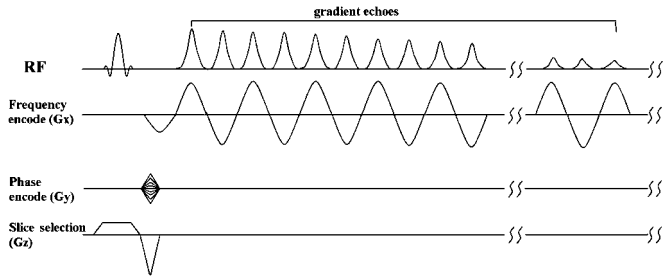


**FIG. 1.** $^{31}$P echo-planar spectroscopic imaging (EPSI) sequence. After a slice-selective 90° RF pulse an oscillating readout gradient is applied which generates a train of 256 pairs of gradient echoes. Each echo is scanned nonlinearly in time at 8 or 16 discrete points.

The application of $^{31}$P EPSI *in vivo* in studies of the calf muscle of volunteers yielded spectra with resolved resonances of PCr and $\alpha$- and $\gamma$-NTP. Figure 4a shows a representative spectrum (TR = 1100 ms, $N = 8$, NA = 64, measurement time 9.4 min) from a voxel of 25 × 25 × 40 mm located in the *M. gastrocnemius*. The signals of PCr [$(S/N)_E \cong 45$, $(S/N)_C \cong 61$] and NTP [$(S/N)_E \cong 3$, $(S/N)_C \cong 4$] are about 25% lower in the EPSI experiment than in CSI with the same voxel size and measurement time (Fig. 4b).

Figure 4c shows an *in vivo* $^{31}$P EPSI spectrum of calf muscle tissue obtained in a measurement time of 20.5 s with phosphocreatine ($S/N)_E \cong 12$ (TR = 640 ms, $N = 8$, NA = 4, voxel size 37.5 × 37.5 × 40 mm). The scan time was shorter by a factor of 2 compared to CSI (TR = 640 ms, NA = 1). With TR = 300 ms (measurement time: 9.6 s) EPSI yielded a signal of $(S/N)_E \cong 7$. Distinct signals could not be detected *in vivo* in EPSI experiments with $N = 16$.

Figure 4d shows the result of a functional $^{31}$P EPSI study with temporal resolution of 20.5 s on the calf muscle of a 25-year-old volunteer. Upon exertion of the muscle (starting at $t = 145$ s) a 40% decrease of the PCr signal intensity was observed.

## DISCUSSION

The data in Fig. 4 demonstrate the feasibility of $^{31}$P echo-planar spectroscopic imaging of phosphorus-containing metabolites in human calf muscle *in vivo*. The technique yields two-dimensional data sets with $S/N$ that permits quantitative evaluation of the PCr resonance in a measurement time that is shorter by a factor of 2 or more than the minimum measurement time possible with CSI. EPSI benefits from the relatively long $T_2$ relaxation time of the $^{31}$P spin in PCr. While EPSI provides better temporal resolution, the $S/N$ of CSI (with the same voxel size and measurement time) is always higher, in agreement with Ref. (*8*). The lower sensitivity of EPSI is expected from the choice of the low-pass filter bandwidth which differed by about 15% from that used at linear data sampling. Moreover, the decline of $S/N$ for increasing DW (Fig. 2a) is explained by the

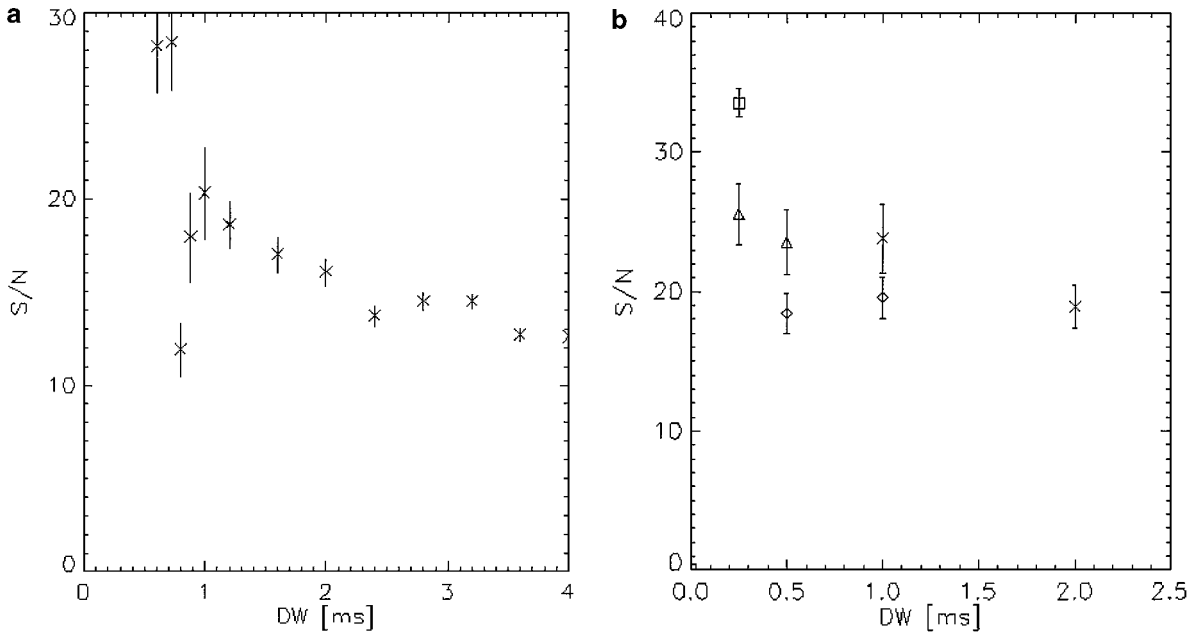


**FIG. 2.** $^{31}$P $S/N$ as a function of dwell time (DW) with (a) EPSI and (b) EPSI with two or four interleaves using gradient rise times $T_{ramp} = 250$ $\mu$s (Δ) and $T_{ramp} = 500$ $\mu$s (◇). For comparison, (b) includes data obtained by EPSI (×) and CSI (□) with the same experiment (model solution: 50 mM PCr). Experimental parameters: measurement time 5.9 min, repetition time TR = 1100 ms, number of phase-encoding steps $N = 8$, number of averages NA = 40, and voxel size = 37.5 × 37.5 × 40 mm.

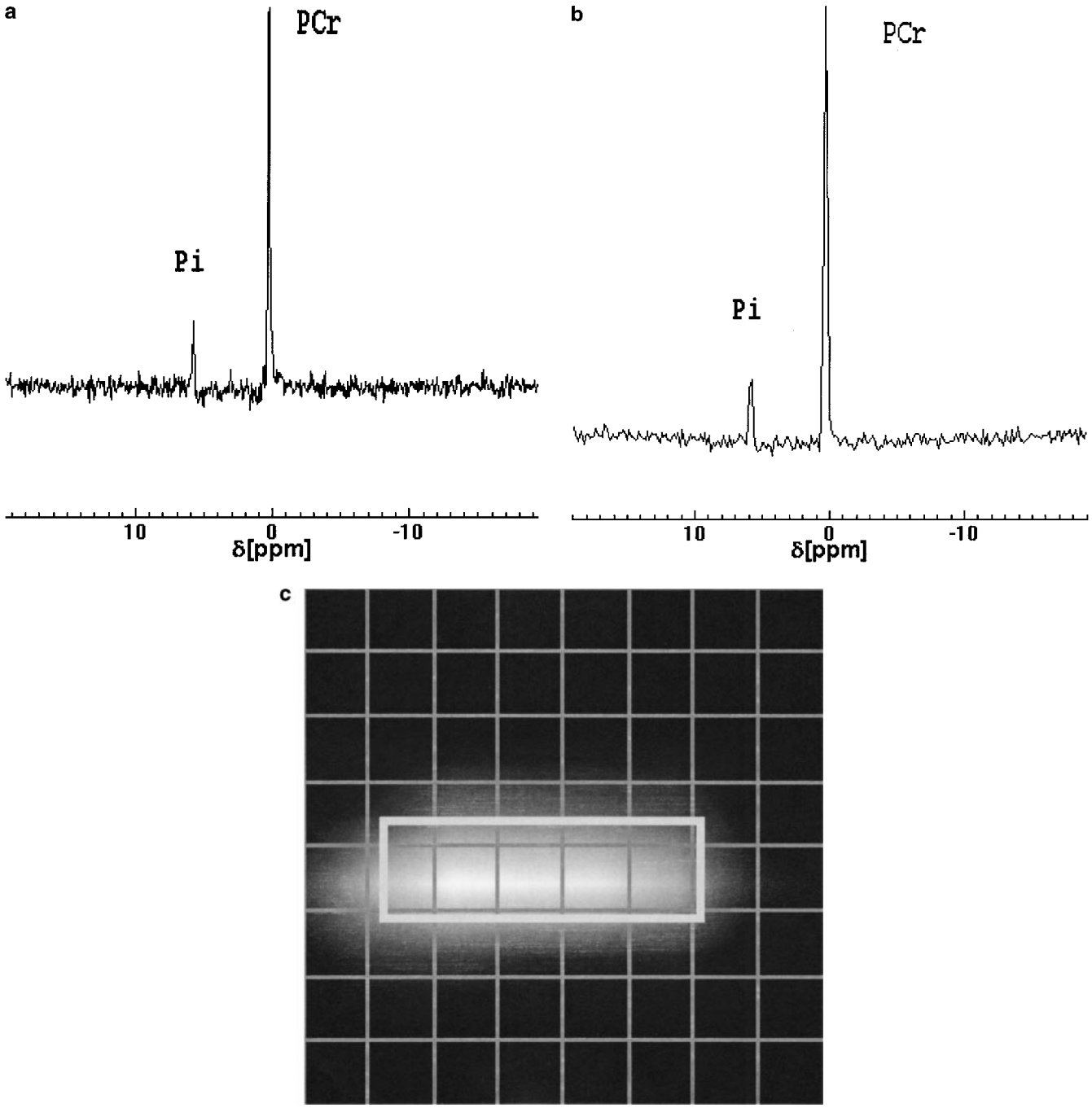


**FIG. 3.** Localized $^{31}$P NMR spectra (measurement time 5.9 min, TR = 1100 ms, voxel size = 37.5 × 37.5 × 40 mm) and spectroscopic image of a cylindrical phantom (50 mM PCr). (a) EPSI with $T_{ramp} = 250\ \mu$s (1 kHz spectral width; $N = 8$, NA = 40). (b) CSI with DW = 250 $\mu$s (4 kHz spectral width; display, 1 kHz; $N \times N = 8 \times 8$, NA = 5). Data processing (a, b): 1K zero-filling, 1.5 Hz line broading, no baseline correction. (c) Transversal $^{31}$P EPSI image (measurement time 9.4 min, TR = 1100 ms, $N = 8$, NA = 64, FOV = (200 mm$^2$)) showing the distribution of PCr intensity and the contour of phantom.

smaller gradient strength at larger $T_{ramp}$ and hence the less effective refocusing of transversal magnetization components. While rapidly oscillating gradients yielded sufficiently large spectral width and better performance of refocusing transversal magnetization, the aliased noise (due to filter adjustments at different sampling rates) is larger compared to spectra obtained with longer $T_{ramp}$. The weak NTP resonances were only detectable in experiments with $T_{ramp}$ in the range of 600 $\mu$s and $<3$ ms. The optimum gradient rise time was about 250 $\mu s$. The resulting spectral width of 1 kHz suffices to cover the spectral range of endogenous phosphorus resonances. If a wider range is required, the application of interleaved EPSI measurements is favorable.

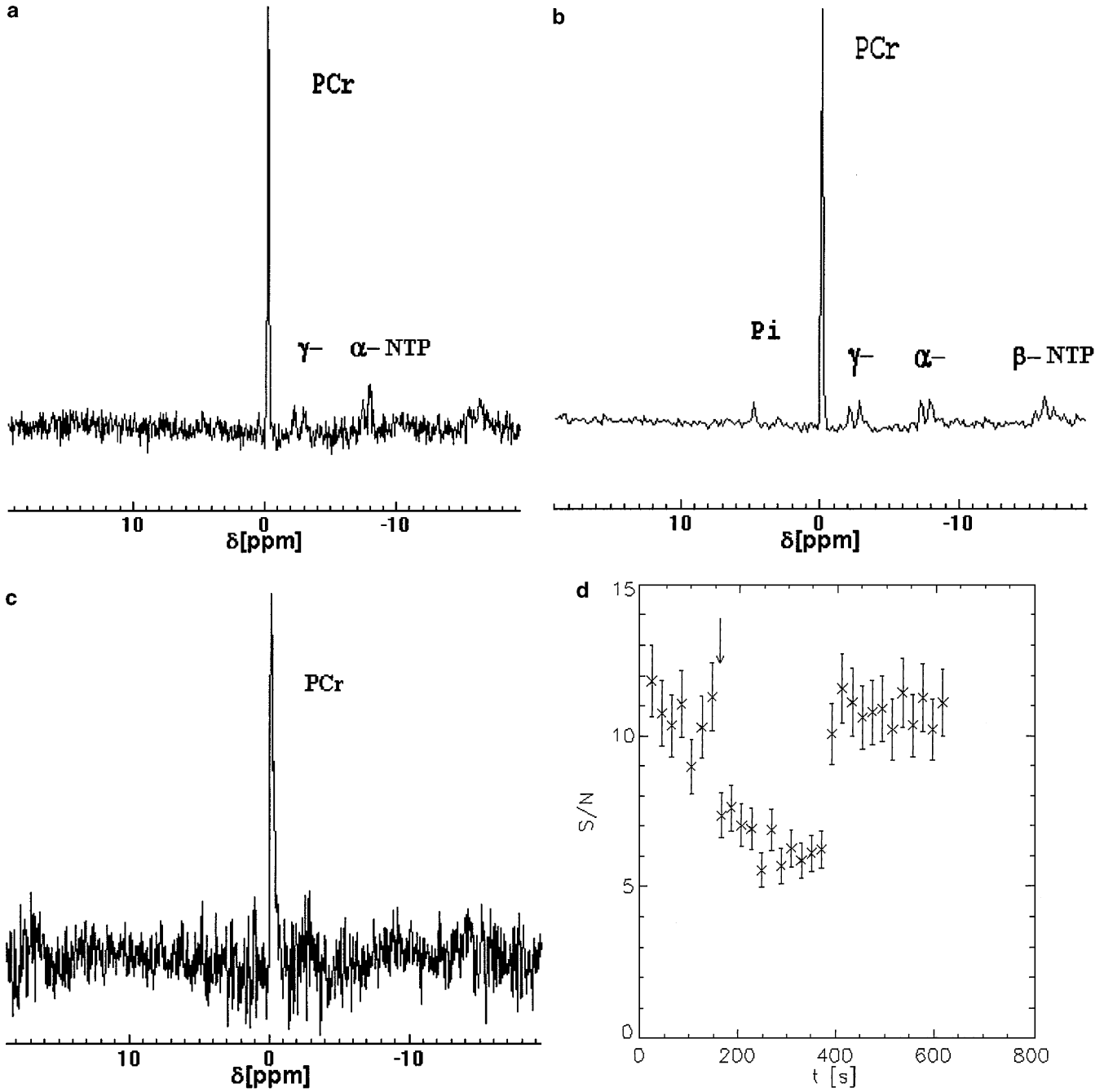


**FIG. 4.** Localized *in vivo* $^{31}$P NMR spectra from the same region in the human calf muscle obtained with (a) EPSI (TR = 1100 ms, $N = 8$, NA = 64) and (b) CSI (TR = 1100 ms, $N \times N = 8 \times 8$, NA = 8). In each experiment, the measurement time was 9.4 min and the voxel size was 25 × 25 × 40 mm. The EPSI spectrum shows resolved resonances of phosphocreatine (PCr) and nucleoside 5′-triphosphates ($\alpha$-, $\gamma$-NTP). The $S/N$ of PCr is 45 in (a) and 61 in (b). Data processing: 1K zero-filling, 1.5 Hz line broading, no baseline correction. (c) *In vivo* $^{31}$P EPSI spectrum of the *M. gastrocnemius* obtained in a measurement time of 20.5 s with $(S/N)_E \cong 12$ of phosphocreatine (TR = 640 ms, $N = 8$, NA = 4, voxel size 37.5 × 37.5 × 40 mm). (d) Functional $^{31}$P EPSI study performed with a time resolution of 20.5 s on the calf muscle of a 25-year-old volunteer (TR = 640 ms, $N = 8$, NA = 4). PCr signal reduction of about 40% upon exertion (start indicated by arrow).

This increases, however, the minimum acquisition time. Since the gradient pulses are the same, interleaved EPSI yields no additional gain in $S/N$ compared to an EPSI experiment of the same scan time.

The application of interlaced Fourier transform to EPSI (*11*) doubles the spectral width, thus rendering EPSI applicable to nuclei with a large chemical-shift range. The method was demonstrated to be robust in combination with *k*-space trajectory

calibration which reduces the imperfections in gradient hardware.

## EXPERIMENTAL

All experiments were performed at $B_0 = 1.5$ T in a whole-body MR scanner (Magnetom Vision; Siemens, Erlangen, FRG). The tomograph is equipped with EPI capabilities providing a maximum gradient strength of 24 mT/m at a minimum sinusoidal rise time of 300 $\mu$s.

$^{31}$P NMR signals were acquired with a planar surface coil (Siemens) of 14 cm diameter. After shim on the tissue water $^{1}$H resonance, $^{31}$P NMR spectra were obtained by means of one-pulse-acquire and multivoxel techniques ($B_1$ inhomogeneity excluded spin-echo excitation). To assess spatial resolution and spectral quality, conventional CSI was performed after the EPSI experiments. For *in vivo* studies the calf muscle of eight previously informed and consenting healthy male volunteers was examined. In functional studies the volunteers performed plantar flexion of the foot pinned down with a 3-kg load to exercise the gastrocnemius and soleus muscles. *In vitro* experiments were performed with a model solution of PCr (50 mM). The phantom had a cylindrical shape with a diameter of 12 cm and thickness of 4 cm.

The 2D EPSI pulse sequence employed is shown in Fig. 1. After slice-selective FID excitation (sinc RF pulse of width $t_p = 1280$ $\mu$s) of $^{31}$P spins in a transversal slice, a phase-encoding gradient pulse (duration $t_G = 1$ ms) is applied, followed by an oscillating gradient during signal acquisition. A slice thickness of 40 mm, a field of view of (200 mm)$^2$, and $N = 8$ phase-encoding steps yield a spatial resolution (voxel size) of $25 \times 25 \times 40$ mm.

The oscillating gradient generates a series of gradient echoes, which are spatially encoded in one direction and which contain chemical-shift information. The gradient consists of 256 pairs of alternating lobes, each with a quarter-sine ramp-up and a quarter-sine ramp-down. Gradient rise times ($T_{ramp}$) in the range of 150 $\mu$s to 1 ms were used. The 256 pairs of lobes correspond to 512 time points at each *k*-space location. Because of nonuniform sampling in time the echoes were separated in even and odd echoes to compensate for imperfections of the oscillating gradient.

The sinusoidal shape of the gradient ramp was taken into account by using a sine-integrated ADC trigger frame for data acquisition, such that nonequidistant sampling points in time yield equally spaced values in *k* space. To reduce imperfections in the system timing an ADC delay time correction was performed prior to the data acquisition. The bandwidth of the low-pass filter was adjusted to the different sampling rates.

In order to increase the spectral width multiple interleaves, offset in time, were employed (*12*). Double and fourfold interleaves were obtained by shifting the gradient pulse train in time by $T_{ramp}$ or $2 \times T_{ramp}$. The result is an increase of spectral width by factors of 2 and 4, respectively. The interleaved experiments were performed with $T_{ramp} = 250$ or 500 $\mu$s.

CSI was performed with the oscillating readout gradient replaced by a phase-encoding gradient, but with the same measurement parameters as in the EPSI experiments. During 256 ms signal acquisition 1024 data points were sampled at 4 kHz spectral width.

Reconstruction of the EPSI data and evaluation of spectra were done offline using SiTools (provided by A. Maudsley, VA Medical Center, San Francisco, CA). After time reversal of the even echoes the two data sets corresponding to odd and even gradient echoes were processed separately by applying spatial Fourier transform. For spectral processing, the data were zero-filled to 1K points, followed by 1.5 Hz Gaussian line broadening and Fourier transformation. The even echo spectra were phase-corrected to match the odd echo spectra and then both data sets were added. This yields a theoretical gain in $S/N$ by a factor of $\sqrt{2}$. The sensitivity was determined according to $S/N = A/(2\sigma)$, where $A$ is the amplitude of the resonance in the Fourier spectrum and $\sigma$ the root mean square deviation from the mean amplitude outside the frequency range of $^{31}$P resonances.

## ACKNOWLEDGMENT

We thank Dr. Andrew A. Maudsley, VA Medical Center and University of California, San Francisco, California, for kindly providing MRSI processing software SiTools.

## REFERENCES

1. P. Mansfield and A. A. Maudsley, *J. Phys. C* **9,** L409–L412 (1976).
2. K. K. Kwong, J. W. Belliveau, D. A. Chesler, I. E. Goldberg, R. M. Weisskoff, B. P. Poncelet, D. N. Kennedy, B. E. Hoppel, M. S. Cohen, R. Turner, H.-M. Cheng, T. J. Brady, and B. R. Rosen, *Proc. Natl. Acad. Sci. USA* **89,** 5675–5679 (1992).
3. R. R. Edelman, P. Wielopolski, and F. Schmitt, *Radiology* **192,** 600–612 (1994).
4. P. Mansfield, *Magn. Reson. Med.* **1,** 370–386 (1984).
5. S. Matsui, K. Sekihara, and H. Kohno, *J. Magn. Reson*. **67,** 467 (1986).
6. S. Posse, G. Tedeschi, R. Risinger, R. Ogg, and D. Le Bihan, *Magn. Reson. Med.* **33,** 34–40 (1995).
7. J. H. Duyn and C. T. Moonen, *Magn. Reson. Med.* **30,** 409–414 (1993).
8. R. Pohmann, M. von Kienlin, and A. Haase, *J. Magn. Reson.* **129,** 145–160 (1997).
9. A. A. Maudsley, S. K. Hilal, H. E. Simon, and S. Wittekoek, *Radiology* **153,** 745–750 (1984).
10. W.-I. Jung, K. Straubinger, M. Bunse, F. Schick, K. Kuper, G. Dietze, and O. Lutz, *Magn. Reson. Med.* **28,** 305–310 (1992).
11. G. Metzger and X. Hu, *J. Magn. Reson.* **125,** 166–170 (1992).
12. L. Hilaire, F. W. Wehrli, and H. K. Song, *Magn. Reson. Imaging* **18,** 777–786 (2000).